Scientific Research and Essays Vol. 7(40), pp. 3368-3381, 23 October, 2012
Available online at http://www.academicjournals.org/SRE
DOI: 10.5897/SRE11.1877
ISSN 1992-2248 ©2012 Academic Journals

Full Length Research Paper

Imaging fractures in a massive limestone with ground penetrating radar, Haymana, Turkey

Aysel Seren* and Aydanur Demirkol Acikgoz

Karadeniz Technical University, Department of Geophysics, 61080 Trabzon/Turkey.

Accepted 9 September, 2012

This study was conducted by utilizing ground-penetrating radar (GPR) to determine the subsurface conditions of the Mollaresul High Plateau located in Haymana, Ankara, Turkey. The site is thought to be managed as a marble quarry. The GPR reflection profiling method was used because it could be applied rapidly and non-invasively without causing any damage to the surveyed area. Approximately N-S directed measurements were collected on 10 profiles using the Ramac CU II GPR system and 100 MHz unshielded antennae. During the data processing stage, the instantaneous amplitude and combined analysis of the phase-group sections were added to the basic processing steps in order to obtain more detailed images of the shallow subsurface in phase-group sections and the energy distribution of the traces in the instantaneous amplitude sections. The conditions of the environment were in the vadose zone and the electrical conductivity of the marble was low. Georadar yielded penetration depths of about 40 and 45 m below ground level. The joint interpretation of the instantaneous amplitude and phase-group sections highlighted strong reflectors, which are indicative of the locations, extensions and sizes of the main fractures in the rock mass. The continuous sub-horizontal reflections found at a maximum depth of 45 m within the marble mass were monitored on the interpreted radargrams to image the extension of fractures. The locations of more massive blocks surrounded by weathered material, low-angle joints and fractured rocks with specific inclinations were also determined. The results highlighted whether the quarries are exploitable or not. With such useful information, unnecessary excavations are avoided and the quarrier gains substantially in terms of time and cost.

Key words: Georadar, instantaneous amplitude and phase group attributes, marble, fracture-crack images, Turkey.

INTRODUCTION

Marble is commonly extracted from quarries and may be used for building and ornamental purposes. Therefore, the main objective of marble quarry exploitation is to extract marble blocks in the required sizes and prevent risk to quarry workers during its extraction. From the quarry operator's point of view, it is fundamental that preliminary geophysical investigation be conducted for proper quarry planning, which will determine where to start extraction work and show the orientation of the quarry faces and benches. As a consequence, geophysicists have adopted the ground-penetrating radar (GPR) method, which makes use of electromagnetic waves and serves such a purpose adequately. Furthermore, GPR is a non-destructive method which displays effectively the shallow subsurface of granitic, marble and similar rock masses at a high resolution. Successful examples of such studies were carried out by Tillard (1994), Grasmueck (1996), Grandjean and Gourry (1996), Seol et al. (2001), Shaffer and Wenning (2002), Tsoflias et al. (2004), Porsani et al. (2006), Jeannin et al. (2006), Deparis et al. (2008) and Kadioglu (2008).

Indeed, they all came to the conclusion that the GPR was

*Corresponding author. E-mail: seren@ktu.edu.tr or aysel.seren@gmail.com. Tel: +90 462 377 27 28. Fax: +90 462 325 74 05.

a successful way of detecting reflector depth and the boundaries between formations having different dielectric properties.

However, natural discontinuities and karst may give rise to problems in the economic exploitation of quarries where industrial extraction of raw material is performed. These problems may also generate unfavorable safety, hydrologic and environmental conditions in quarries with voids and fractures. The GPR technique, which has been used to identify the properties causing such situations and predict the probability of their existence, has been widely accepted as beneficial to the exploitation of quarries (Shaffer and Wenning, 2002). Moreover, it has been shown that structural discontinuities and fracture distribution play an important role in the localization of high quality granite (Porsani et al., 2006). Such information is essential in mining engineering because it will guide the quarry operator in the planning stage and help to minimize costs. Indeed, starting quarrying activity without having any information about the conditions of the subsurface does not guarantee good results. As the purpose of a quarry manager is to make profits, it would be costly and time-consuming to conduct excavations before identifying the structural discontinuities of the subsurface because the marble may not be massive and not suitable for commercialization.

In this survey, ground-penetrating radar was used in order to map the fracture distribution and joints between the strata situated in the study area. The area, 40 × 50 m^2, was located at Mollaresul High Plateau in the district Haymana (Ankara), in Turkey. It was surveyed with a view to determining whether the area was suitable for marble quarrying or not. The site needed to have characteristics such as a good outcrop control to verify results, non-conducting near-surface conditions so that a minimum of 40 m penetration depth could be obtained, and geological structures with length scales of about 1 m with the approximate wavelength of a 100 MHz antenna. In this study, instantaneous amplitude and combined analysis of the phase-group were used in addition to basic data processing methods. Instantaneous amplitude and combined analysis of the phase-group were utilized to determine the energy distribution of the traces in instantaneous amplitude sections. As a result, we obtained more detailed images of fracture networks in phase-group sections.

The instantaneous amplitude or envelope is a measure for the reflectivity strength, which is proportional to the square root of the complete energy of the signal at an instant of time. The envelope gives an overview of the energy distribution of the traces and, on the other hand, it can facilitate the detection of first signal arrivals (Sandmeier, 2009). The subvertical and lateral continuity of boundaries generated by high amplitude reflections was sounded by examining the effectiveness of these complex trace analyses on the georadar results. The purpose of this study is to delineate the images of fractures and structures in strong marble by using complex trace analysis. The benefit of applying complex trace analysis on GPR data is that it enhances the resolution of fractures and cracks in the radargrams.

Geology of the study area

The study area is located at Demirözü Village (Haymana), 120 km far from Ankara in Turkey (Figure 1a) around Mollaresul High Plateau. The geology of the proposed marble quarry site consists of the Triassic Temirözü formation, the upper Jurassic to lower Cretaceous Mollaresul formation, the Paleocene Kartal formation, the Miocene Kırkkavak formation, the Neogene clastic sediments and alluvium (Ünalan et al., 1976) (Figure 1b). The Triassic Temirözü formation comprises sedimentary rocks consisting of limestone and greywacke. This lithology is un-conformably overlain by the Upper Jurassic to lower Cretaceous Mollaresül formation. This formation comprises a greyish, medium-thick and massive bedded limestones. The Paleocene Kartal formation, unconformably overlies the carbonate rock and is dominated by clastic sedimentary rocks. This unit contains layered conglomerates, sandstones, marls, claystones and mudstones. Whilst the limestones are cemented, the mudstones are generally poorly consolidated, depending on the conditions at the time of deposition. The Paleocene series are unconformably overlain by the Miocene Kırkkavak Formation, which is primarily composed of algal limestones and grey marls. All lithologies in the study area are unconformably overlain by sandstones and marl, and alluvium of quaternary age. The rocks in the area of investigation have been affected by regional tectonic phases. Very fractured parts and associated structures have been observed in these rocks, especially on the north of Türbe Tepe, where most of the rocks are covered with the youngest lithologies (Acıkgoz, 2008).

METHODOLOGY

Ground penetrating radar

GPR is a non-destructive, non-invasive geophysical method that produces a continuous cross-sectional profile. GPR profiles are used to evaluate the location and depth of buried objects. They are also useful tools for investigating the continuity of natural subsurface conditions and presence of features. This method operates by sending pulses of high frequency electromagnetic waves down into the ground through a transmitter antenna. A receiver antenna then receives the reflected waves from various distinct contacts and stores them in the digital control unit, which registers the reflections against two-way travel time in nanoseconds. The output signal voltage peaks are plotted on a

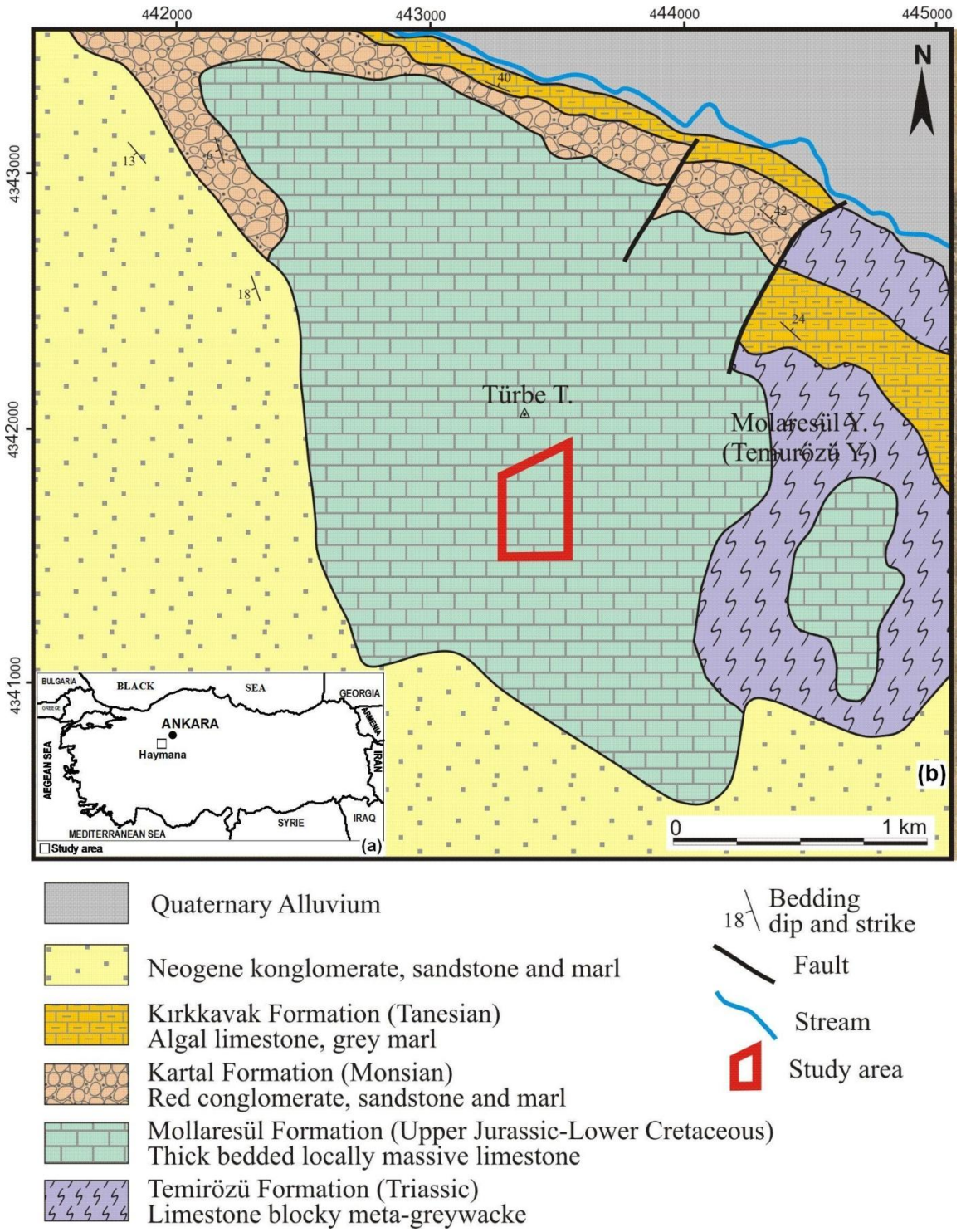

Figure 1. (a) Map of Turkey and geographical location of Haymana, (b) Geological information of the study area.

GPR cross-sectional profile (Daniels, 2004) (Figure 2). The energy reflected on a discontinuity between two different dielectrics depends on the reflection coefficient. Assuming that the conductivity of the medium is low, this coefficient is a function of the incidence angle of the radar wave and the permittivity contrast on either side of this discontinuity (Davis and Annan, 1989). For standard permittivities (Olhoeft, 1981) and for normal incidence, this coefficient is 0.42 for a reflection between marble and air, assuming relative permittivities of 6 and 1 for marble and air respectively; values fall to -0.57 between marble and water, and

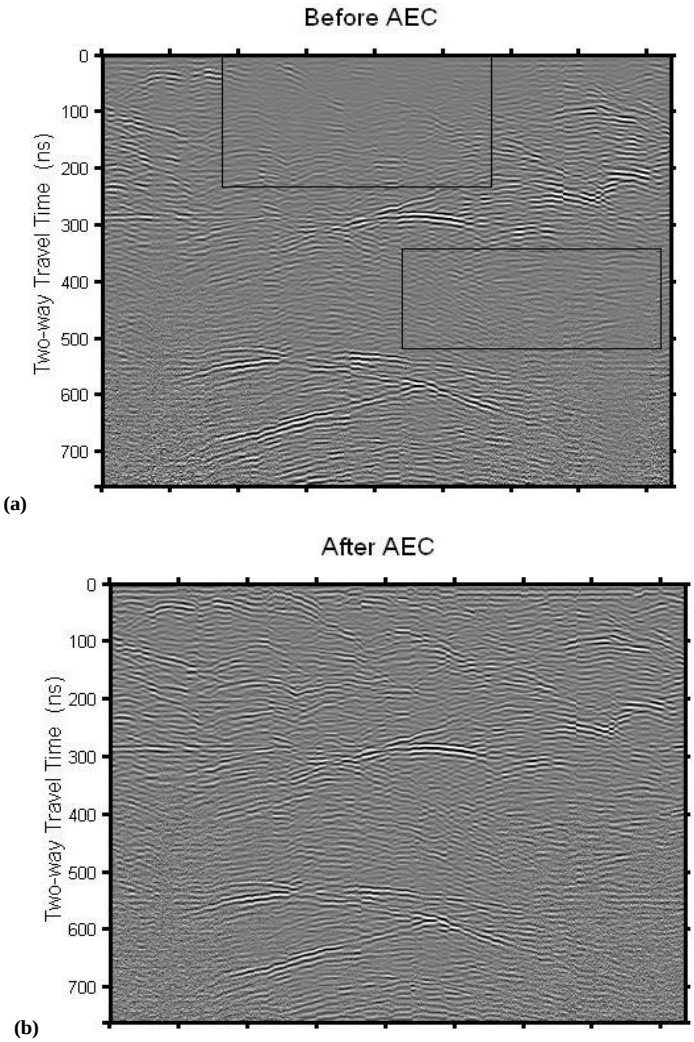

Figure 2. (a) Processed data with only Energy Decay (without AEC) and (b) Processed data with Energy Decay and AEC.

-0.12 between marble and shale. If fractures are sufficiently open and filled with air or water, as in the case of karst, the amount of energy returned will be high, and will therefore be recorded successfully. In that case, we identify the fractures by the properties of their content in terms of nature of air, water and size (Grandjean and Gourry, 1996).

Complex-trace transformation

By using amplitude and phase information, traces can be expressed as:

$$S(t) = R(t)\mathrm{Cos}\left[\theta(t)\right] \quad (1)$$

Where R(t) is the envelope and $\theta(t)$ is the time-dependent phase information of the trace, both of which can be determined from the trace S(t) by Hilbert transform. Rewriting Equation 1 to obtain the envelope and normalized phase of the trace, the following equation could be derived:

$$S(t) = R(t)F(t) \quad (2)$$

Where F(t) is normalized phase or the cosine of the instantaneous phase $\theta(t)$ and can be expressed as:

$$F(t) = S(t)/R(t) \quad (3)$$

Decomposition of traces into amplitude and phase traces causes no information loss because the actual trace can be reconstructed by linear multiplication of R(t) and F(t), according to Equation 2. The envelope is a positive-valued trace; however, one can convert the envelope trace to an oscillating time series with both positive and negative values similar to the input trace. To do this, the low-frequency component b(t) is computed, for instance as a running average within a given-time window, T_w, and subtracted from R(t) as follows:

$$g(t) = R(t) - b(t), \quad (4)$$

The result of the reconstruction is the so-called group trace (Shtivelman et al., 1986; Karsli, 2002; Karsli et al., 2006). The determination of the time window length T_w is important. In effect, it has to be selected in such a way that the results are optimum, in other words, without causing any significant loss in the amplitude of reflection waves. This is well illustrated in Figure 3a and b for a simple wavelet. After several tests and applications in this study, we have achieved satisfactory results with the following criterion for the selection of T_w:

$$(N/8)\Delta t \le T_w \le (N/4)\Delta t, \quad (5)$$

Where N is the number of data samples per trace and Δt is time sampling interval. Traces can be decomposed into their normalized-phase and group-trace components and can then be reconstructed to be compared with the input trace as follows (Shtivelman et al., 1986):

$$h(t) = g(t)F(t), \text{ for } g(t) > 0 \quad (6)$$

$$h(t) = 0, \text{ for } g(t) \le 0 \quad (7)$$

Here, the main idea is that zero and negative parts of g(t) trace correspond to side lobes and low-frequency random noise components of the trace, because g(t) trace is calculated by subtracting the b(t) from R(t). Therefore, the omission of zero or negative values in the g(t) trace can improve the temporal resolution and decrease the low-frequency random noise level in the GPR data. So, Equations 6 and 7 provide the reconstruction of the final GPR traces, which are traces with minimized side lobes emphasizing the main common features of the original trace by using their normalized phase and group traces. The results showed that combined analysis of the phase-group section for specific conditions give complete and reliable information about the content of GPR data according to original sections. This process is simple and it also does not require much mathematical computation, and the only parameter selection required is T_w. In addition, it allows the researcher to identify irregularities of complex subsurface and clearly indicates heterogeneous parts appearing on the input section with respect to near surface and basement.

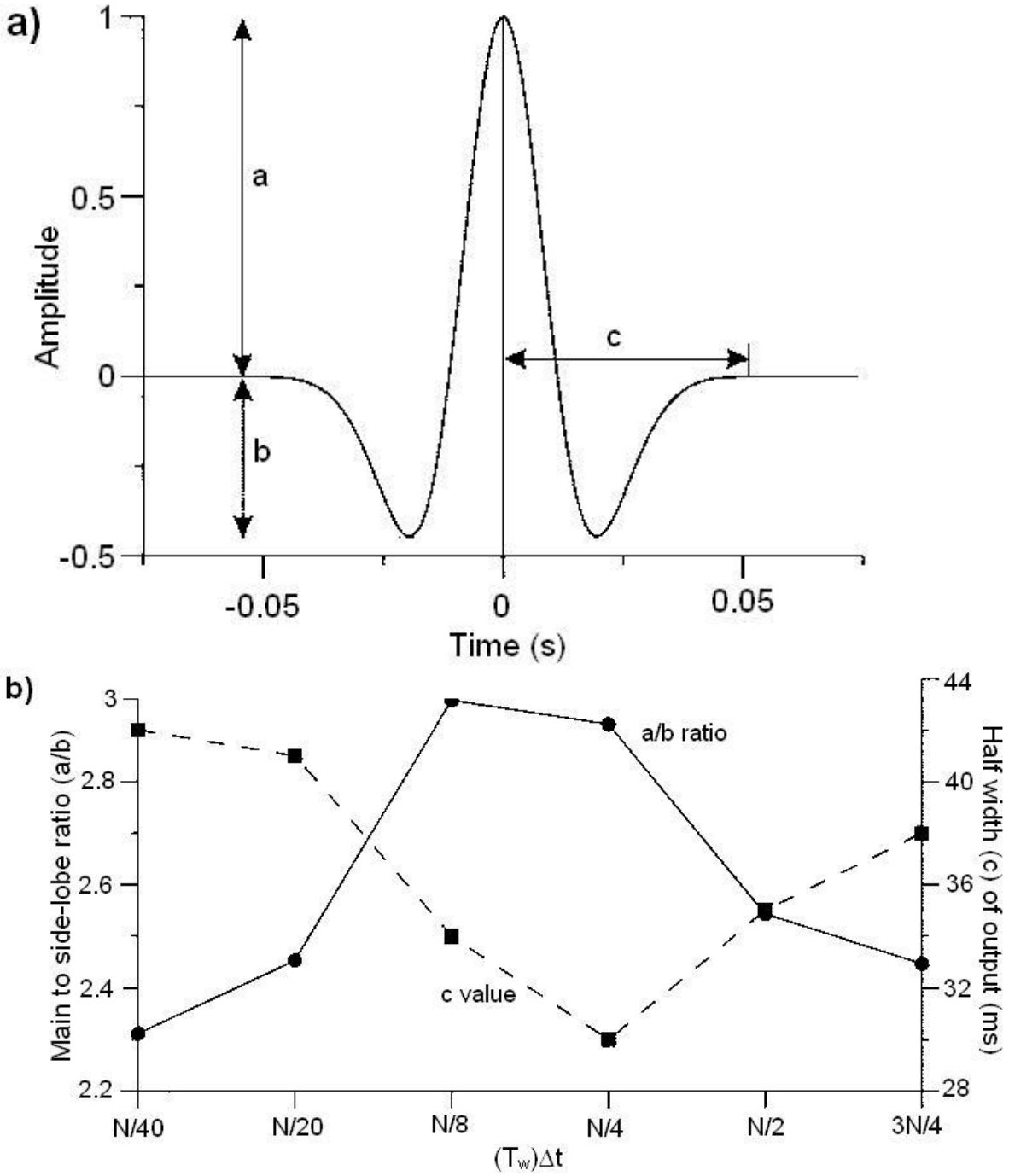

Figure 3. The effect of the method both in amplitude and temporal width of the input. (a) Input 20-Hz Ricker wavelet without noise and its parameters, a: main-lobe amplitude, b: side-lobe amplitude, and c: half-time width; (b) Trade-off between main- to side-lobe amplitude ratio (a/b) and the change in the half-width of the output for different Tw values (Karsli et al., 2006).

Data acquisition

The Ramac CU II GPR system was used with 100 MHz unshielded antennae (Figure 4), with a depth resolution of about 0.2 to 0.25 m according to an electromagnetic wave velocity of about 0.08 to 0.12 m/ns. The offset between the transmitter and receiver antennae was 1 m. The study area was a horizontal platform of about 2000 m^2. Ten profiles in N-S direction were selected in the investigated site (Figure 5a and b). These profiles were acquired with spacing changing from 2.8 to 9.4 m. The length of the profiles was about 40 to 45 m (Figure 5a). The profiles were taken perpendicular to the visible fractures on the surface, as documented by Tsoflias et al.

Figure 4. Ramac/GPR CU-II with 100 MHz antennas (transmitter and receiver) at starting point of Haymana profile.

(2004). Trace spacing was 0.1 m, and the total time window was 761.913 ns, with 0.918 ns of time sampling interval per trace on each profile. Reflections were detected from depths of about 40 to 45 m using the Ramac CU II GPR system with 100 MHz unshielded antennae. The penetration depth was enhanced owing to the dry conditions of the domain and low electric conductivity properties of the marble. It was possible to obtain a constant velocity of 0.12 m/ns for all the profiles due to the relative homogeneity of the marble and the velocity of the marble varied between 0.115 and 0.128 m/ns (Grandjean and Gourry, 1996). That velocity was a root-square-mean velocity, which was estimated by fitting hyperboles associated with diffractions and caused by vertical fractures. Time–depth conversion was performed using a velocity equal to 0.12 min. The penetration depth does not only depend on the frequency of the antennae, but also on the electromagnetic characteristics of the rocks present in the site. GPR signals can reach depths of up to 50 m in low conductivity materials such as dry sand, granite or marble (Jol, 2009: 46). Moist clays, shale, and other high conductivity materials may attenuate or absorb GPR signals, which greatly decrease the penetration depth to 1 m or less. The depth of penetration can also be determined by GPR antenna frequency. Antennas with low frequencies of 25 to 200 MHz obtain subsurface reflections from deeper, but with lower resolution. These low frequency antennas are used for investigating the geology of a site, such as locating sinkholes or fractures, and locating large and objects buried deep (Davis and Annan, 1989; Daniels, 1996; Annan, 2003). It is difficult to recognize or interpret GPR signals from deeper reflectors. Therefore, some imaging processes may have to be applied to the GPR data to make these signal amplitudes of deeper reflections more visible. One of these basic processes is Energy Decay, which is widely used in georadar studies. Visibility of GPR signals gained by Energy Decay can be further enhanced by another technique called the Amplitude Envelope Correction (AEC). The AEC gain function was computed and applied after energy decay. It was firstly computed as a Hilbert Envelope of the input trace, secondly the envelope was smoothed by convolution process using a triangular smoother window function, and finally, the AEC result trace was obtained by dividing the input GPR trace by the smoothed envelope.

The Energy Decay and AEC process yielded acceptable results and provided us with more interpretable GPR images (Figure 2a and b). Comparing Figure 2a with 2b, it is clear that better visibility was obtained after AEC processing, especially in the selected parts (see boxes). However, complex geological structures such as fractured parts, magmatic rocks, karst, etc, may cause problems in the interpretation of GPR data. The wavefields in such media have a complicated interferential (of or pertaining to interference especially of waves or signals) character and should be considered as consisting of complex wave groups defined by their phase-group properties (Gelchinsky et al., 1985). These features depend on both the characteristics of the medium and geometry of the recording system and may differ considerably from each other. These properties can be studied by defining a GPR trace as a real part of a complex function time as discussed by Shtivelman et al. (1986). This process was also successfully applied to GPR data due to their similarity to seismic data by Patterson and Cook (2000). These researchers stated that when carefully used in conjunction with good knowledge of the geological conditions, the method promises to provide an important tool for mapping internal structures of pegmatites, which is essential for future mining activities. Therefore, the authors believe that the study area, which consists of massive limestone (Figure 1b), is suitable for marble exploration with this method.

Data processing

It is difficult to observe the condition of subsurface structures from raw GPR profiles. Therefore, it is necessary to process the data so that they can be more easily interpreted. In this study, the basic data processing steps consist of Energy Decay, Dewow, Subtract DC shift and Background Removal. Application of static correction (this means a time-independent correction for each trace in time direction) to the data was not required because the topography of the study area was flat. In addition, there were no sources of artificial noise in the vicinity of the area, which enabled us to acquire high signal to noise ratios. One of the data processing steps, Energy Decay, is a filtering technique used to compensate for the decrease in amplitude due to the distance of propagation of the electromagnetic wave within the domain. A ratio decrease was calculated from all the traces in the measurement profiles during this process. Then, with this energy decay recovery, each trace amplitude adjustment was performed by dividing the amplitude value of each point. A defined increase in amplitude is caused by this filter going downward over the trace because the waves lose more energy while propagating to greater distances within the ground.

Another data processing step applied in this study was the Dewow. Dewow consists of the removal of low frequency waves from the traces. While performing this task in mathematical terms, the selection of the time window is of great significance with respect to the running mean value. Because this filter can remove useful data, the user's attention during this process is required. The zero mean, also known as the subtract DC shift, is a constant shift taking place over time (Arcone et al., 1998). The final data processing application, known as Background Removal, has been accepted as an important step in the analysis of GPR. The ringing effect, a common type of coherent noise, is observed in the GPR data and has a negative impact on the radargram signals (Annan, 2003). If this type of random noise is strong and not properly removed, deeper features may be completely masked. Therefore, ringing, which is regarded as horizontal and periodic events in the sections, is one of the most significant phenomena to be eliminated with data processing. Given that the ringing effect is nearly consistent along the whole section when reflected events are less correlated and

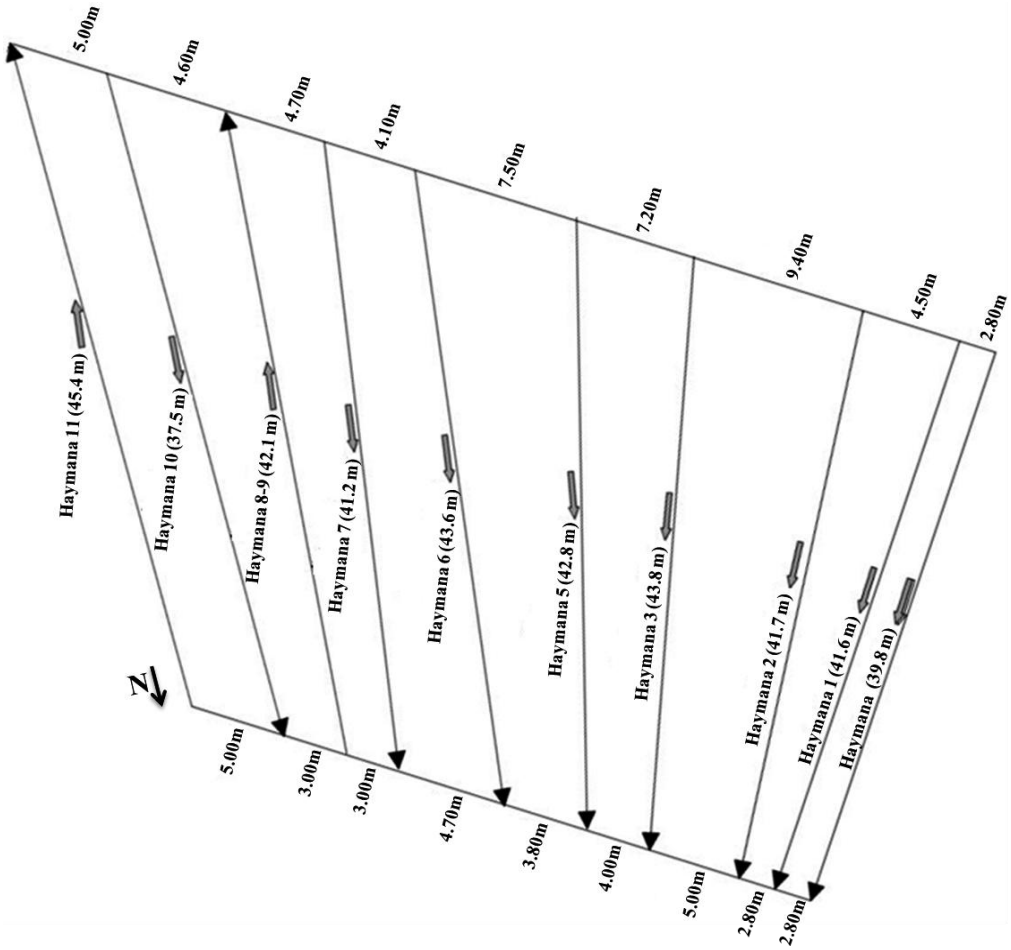

Figure 5(a). Positions of measurement profiles: Names, lengths, directions of the profiles and spacing distances between the profiles.

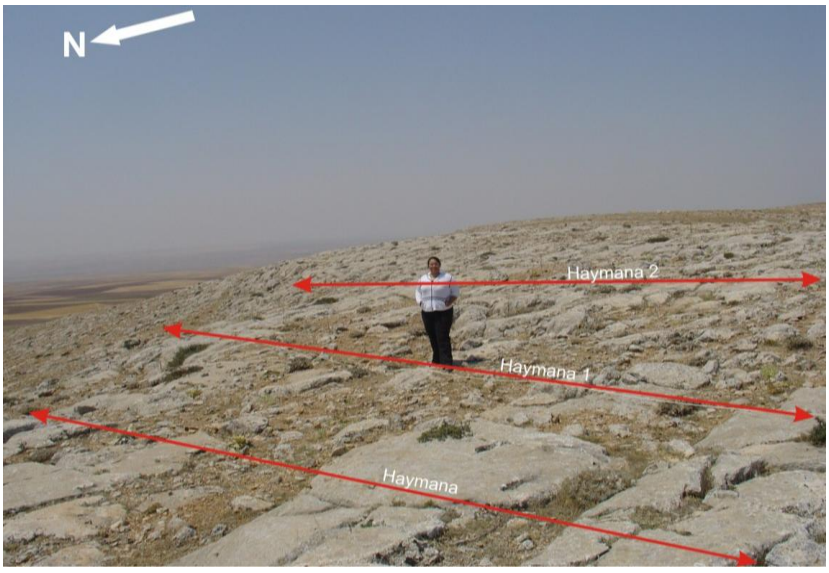

Figure 5(b). A view of the site; some profiles and characteristics of the surface (fractures, cavities weathering).

more random, we can consider the average trace containing ringing noise only for the whole section. Thus, it can be concluded that removing the average trace in a simple way compensates for the horizontal appearance of the ringing in the radargram (Kim et al., 2007). The basic data processing steps of this survey were applied to the data with ReflexW software. ReflexW is a program for the processing and interpretation of reflection and transmission data (special applications: ground-penetrating radar, reflection seismic, refraction seismic and ultrasound) (Sandmeier, 2009). The resulting data were first adapted to the format of this program and then went through the basic data processing steps so that they became interpretable.

However, the migration processing step was not considered to be relevant in this study because 2D migration processing made small-scale vertical fractures invisible (Grasmueck et al., 2005). Besides, it has been shown that strong reflections could be limited by unmigrated GPR data visualization (Kadioglu, 2008), which was not the case in our study since the obtained hyperbolas were not very large.

RESULTS

GPR reflections on the profiles of this paper showed detailed images of inclined and sub-horizontal reflectors to approximately 40 $\pm$ 5.5 m depth, as well as shallow diffractions (yellow lines in figures a of the profiles). The prominent fractures are frequently associated with high energy reflections of electromagnetic signal (Orlando, 2003). On profile Haymana 1, from right to left (as indicated by the box), a dense fracture network has been observed in the site between depths of about 4 and 16 m (Figure 6a). On instantaneous amplitude and the phase-group sections of this radargram (Figure 6b and c), strong reflectors extending sub-horizontally have been identified. Figure 6a shows strong reflections between about 18 and 23 m depths and between distances of 9 and 28 m as indicated by the yellow lines. Another strong reflector is found between approximately 36 and 42 m depths. Besides, the strong reflectors detected at the observed depths are also present in the phase-group and instantaneous amplitude sections. The box on the right of the interpreted radargram of profile Haymana 5 reveals a fracture network between depths of about 9 and 32 m and distances of 36-43 m (Figure 7a). Additionally, in this radargram, horizontally oriented and inclined strong reflectors which are indicated with continuous lines have been observed at 4 and 30 m depths. The observed excess in reflectors having high amplitude, especially in the GPR sections obtained from profiles Haymana 10 and 11, can be considered as an indication of fractured parts (Figure 8).

The studied profiles were taken on the Late Jura-Early Cretaceous Mollaresül Formation. Because this formation is composed of one of the oldest units in the region, it has been affected by tectonic activities over a long period of time and it has acquired a fractured structure. In-situ observations show that these units are made of thick and massive limestone layers. In addition, vertical fractures have been observed at the surface within units and in neighboring quarries during field study (Figure 9a and b). Surface cavities have also been detected on carbonates in places (Figure 9c). As shown in the geological map, the profiles are nearly N-S oriented (Figure 5b). The limestones in the Mollaresül formation are approximately oriented E-W and dipping to the North at an angle of 15 - 20° (Figure 9c).

DISCUSSION

In this study, the combined analysis of phase-group attributes, which is a method used in the evaluation ofreflection data, was applied to GPR data to investigate a marble site. This approach has proved effective since it has yielded images with improved resolution. The results acquired by application of complex trace analysis to GPR data were compared with the radargrams obtained after the basic data processing steps. The instantaneous amplitude sections were also used to display the energy distribution of the traces as shown in the figures of all the profiles. The reflectors which are visible on Haymana 1 correspond to subhorizontal fractures dipping to SW and subhorizontal fractures dipping to NE. Comparing the sections of Figure 6a, b and c, it can be concluded that the phase group sections have produced images at a higher resolution (see circles).

In Haymana 5, it can be concluded that the reflectors found in the boxes (Figure 7a) correspond to fractured parts. The fractures in question have provided strong reflections that are easily noticeable in the instantaneous amplitude and phase-group sections (Figure 7b and c). When the interpreted section of this radargram (Figure 7a), instantaneous amplitude and phase-group sections are assessed together, details which are particularly visible in the phase-group section (see circles) and are not displayed by the other sections can be identified. The horizontal reflections with high amplitude in the interpreted GPR sections may be caused by bedding plane of the surface, whereas the dipping reflections are thought to be induced by extension fractures. The pronounced lineation in some parts of the sections (Figure 7a) may be due to karstic cavities or different lithologies in these discontinuities.

In this study, complex trace analysis has been used to improve the resolution on the radargrams in general, and not to show the presence of the main fractures only. The authors wanted to show the difference between Figures 6a, b and c, 7a, b and c in the resolution of fractures that can be shown with a 100 MHz antenna (the purpose was not to compare the circled areas with the other parts of the same figure). It is obvious that the radargrams obtained after complex trace analysis (Figures 6c and 7c) generally show a better resolution compared with the radargrams before complex trace analysis; some of the

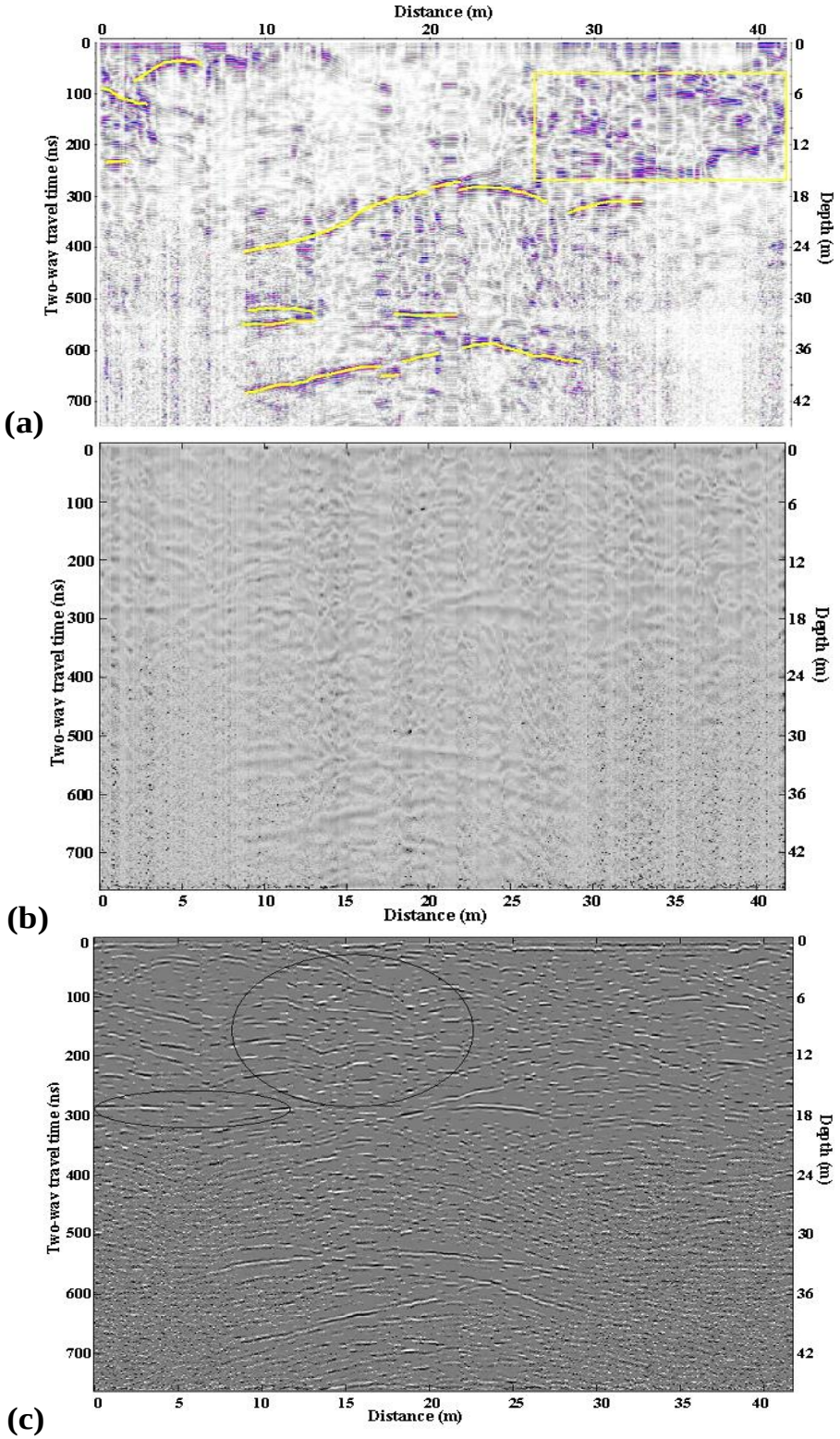

Figure 6. (a) Interpreted fractures of radargram of profile Haymana 1 indicated by yellow lines. The box in radargram (a) indicates a dense fracture network, (b) Instantaneous amplitude and (c) phase-group section of the profile where some of the most significant parts have been circled to show the difference in resolution between radargram (a) and radargram (c).

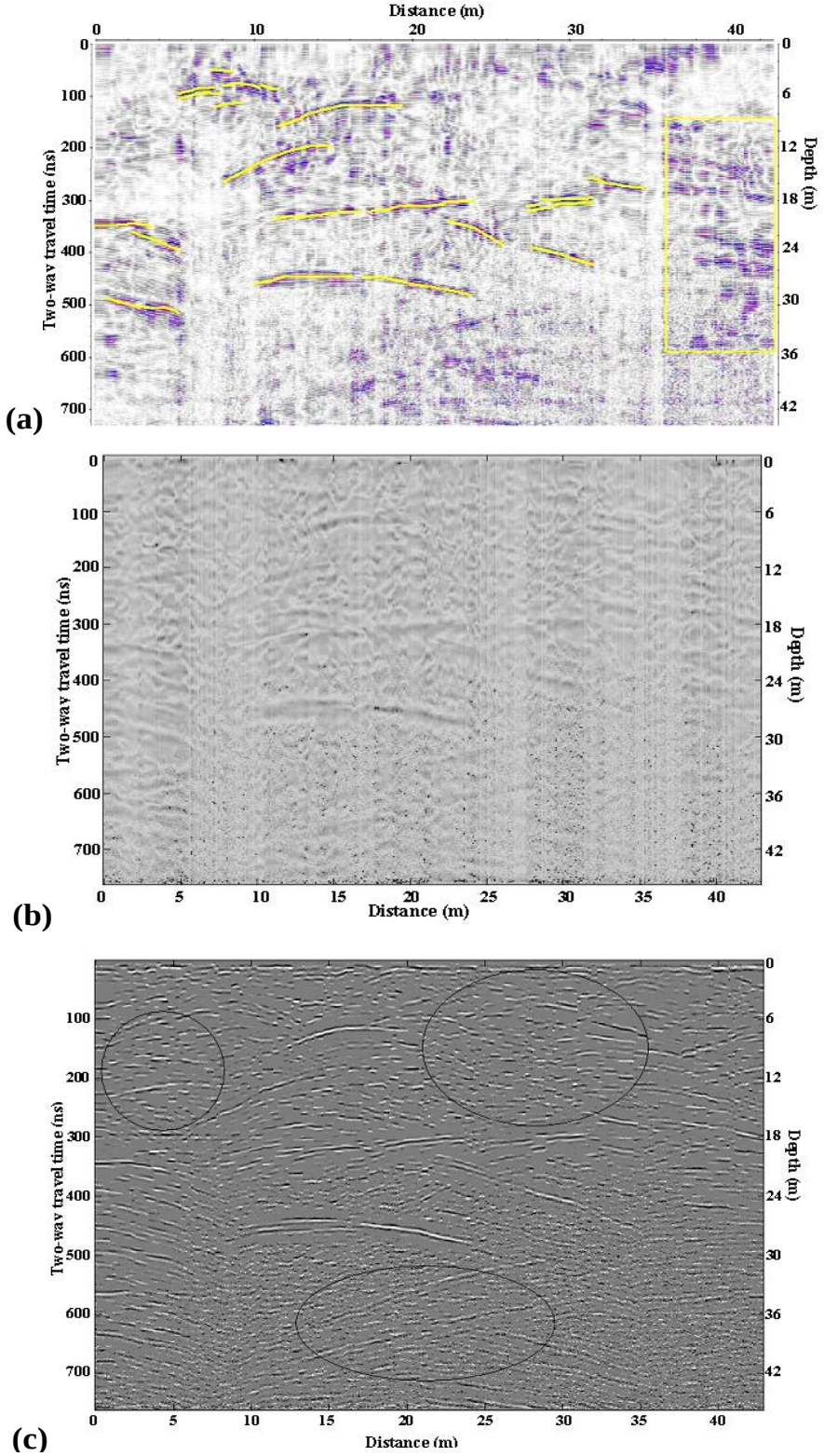

Figure 7. (a) Interpreted fractures of Radargram of profile Haymana 5 indicated by yellow lines. The box in radargram (a) indicates a dense fracture network, (b) Instantaneous amplitude and (c) phase-group section of the profile where some of the most significant parts have been circled to show the difference in resolution between radargram (a) and radargram (c).

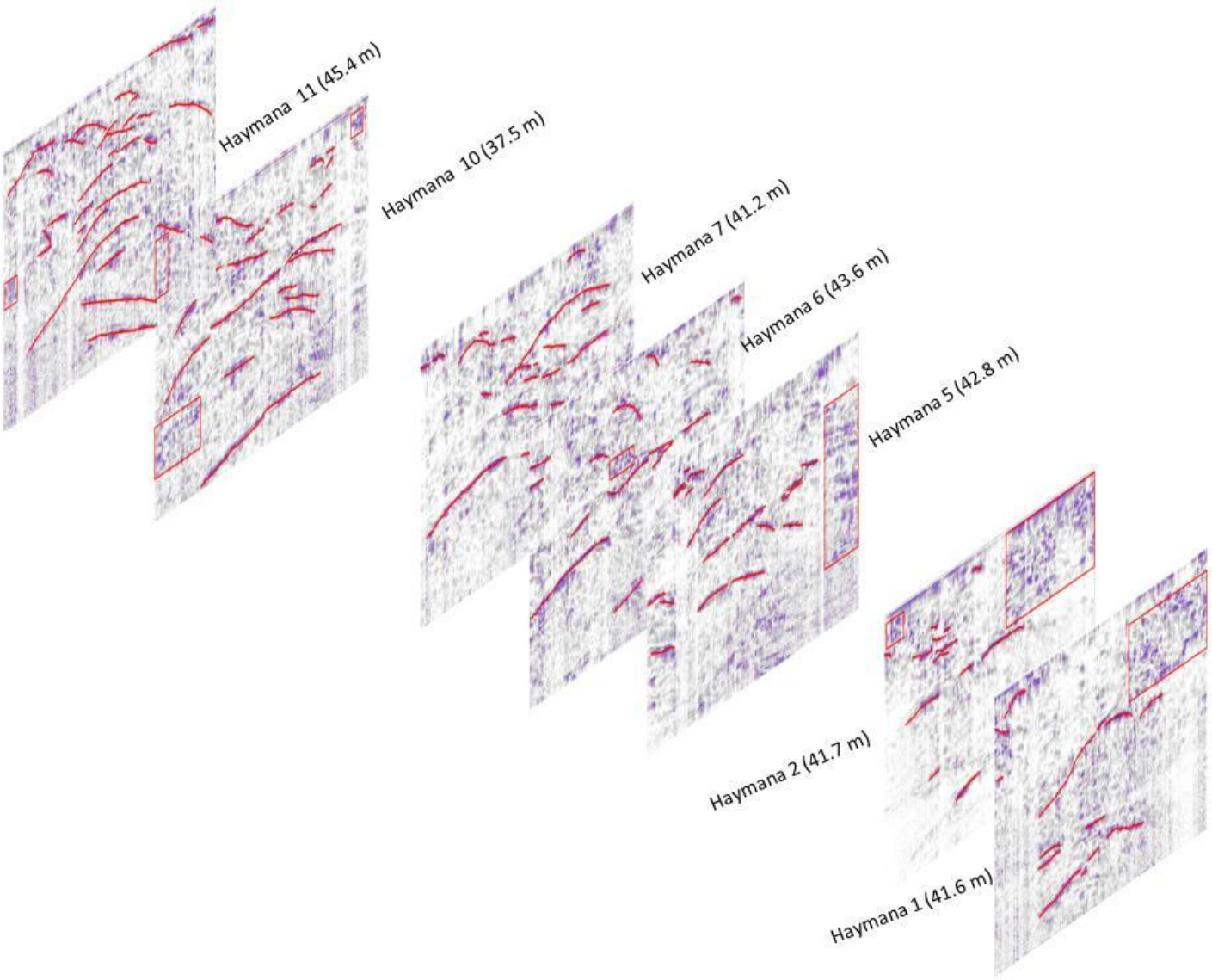

Figure 8. The distribution of structural discontinuities indicated by red lines on all radargrams.

most significant parts were shown with ellipses/circles as examples of better resolution. These parts were not clearly displayed in the radargrams before complex trace analysis (Figures 6a and 7a).

In addition, we have attempted to design a probable model of the subsurface geometry by positioning all the radargrams according to the directions of profiles. From the general outlook of the radargram obtained from 7 N-S oriented profiles, it has been understood that a fractured structure is present in the domain. The observed excess in reflectors of high amplitude, which are especially visible in the GPR sections obtained from profiles Haymana 10 and 11, can be considered to be indicative of fractured parts (Figure 8).

Conclusions

In the site located in Demirozu, a village of the District Haymana (Ankara), in Turkey, a network of fractures and associated rock mass discontinuities were detected using the GPR method. In addition to the basic processing steps, the researchers utilized complex trace analysis, a method commonly used for seismic traces. They applied it to GPR data so that signal to noise ratio was increased and the precision of the interpretation enhanced. The phase-group sections have yielded images with improved resolution as shown in Figures 6c and 7c. On the other hand, the instantaneous amplitude sections revealed the energy distributions (Figures 6b and 7b). As a

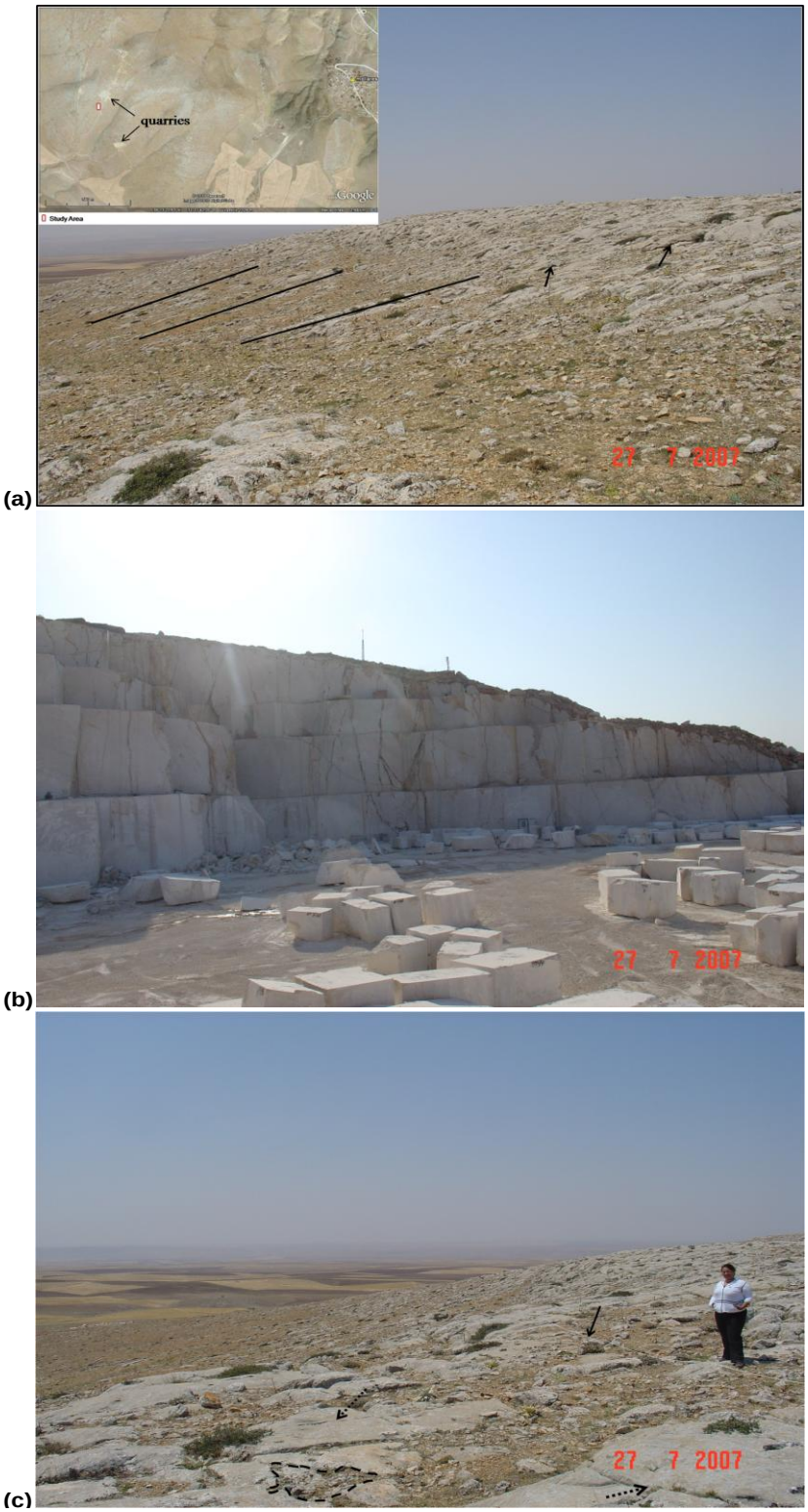

Figure 9. (a) A general view from the site showing the orientation of the bedding (black lines) and surface fractures (arrows), and an aerial photo showing the location of the study area and nearby quarries, (b) A view in a neighboring quarry and the fractured structures and (c) Measurement direction (black arrow), surface cavities (dashed line) and fractures (dashed arrows) on carbonates in places.

consequence, this corroborates that the processed radargrams have given more reliable results about the locations, sizes and directions of the fractured blocks. Sound marble blocks, the parts which have low-angle joints, the networks of fractures and their directions have been effectively localized on the profiles. In this survey, which was carried out with 100 MHz antennae, the penetration depth was provided in places between approximately 40±5.0 m owing to the dry conditions of the domain and low electric conductivity of the marble. As a result, it was possible to delineate the reflection boundaries along the profile, which helped to localize the fractured parts. Besides, three pronounced reflectors were detected around depths of 10 - 12, 18 - 20 and 30 - 35 m in the site. These reflectors may be extension and shear fractures induced by tectonic movements.

Some of the processed and interpreted radargrams of the investigation area are shown in Figures 6 and 7. The reflection surfaces of the subsurface can be identified along the profiles in the radargrams. Furthermore, many diffraction patterns (hyperbolas), a number of near-vertical faults and a system of subhorizontal fractures were visible between stations 4 and 35 m, while there were a few diffraction patterns between stations 0 and 6 m in all the profiles (Figure 8). Absence of reflectors between positions 0 and 6 m could be caused by relatively massive marble, while better resolution and diffraction patterns at the end of the profiles could be linked to fractured blocks of marble. On the other hand, from the obtained radargram, it has been possible to interpret three sets of structures: subhorizontal fractures dipping to SW, subhorizontal fractures dipping to NE, and subvertical fractures.

In-situ observations showed that the limestone has a fractured structure, which has become more noticeable because of surface weathering. Detailed observations in the neighboring quarry also revealed the presence of horizontal bedding, the thickness of which varied between 0.5 and 1 m (Figure 9a and b). Field investigation into the quarry surface indicates that because the bedding and fracture plane disappears between 3 and 5 m, the rock block acquires a massive appearance (Figure 9b). As a consequence, it can be concluded that dipping discontinuities of the GPR sections are not bedding, but are more likely to be extension and shearing fractures induced by tectonic movements as shown in the quarry surface. Besides, observation of the quarry surface reveals parallel extension fractures that are visibly predominant in the upper parts of the quarry surface, whereas shearing fractures are more common in the lower parts of the quarry surface. These observations corroborated by the GPR images. It has been understood that because limestone outcrops have carried various traces (dissolution cavities caused by meteoric conditions as shown by the dashed line in Figure 9c), these rocks have gained a fractured structure over time. Geological observations showed the presence of faults, which have resulted from tectonic movements on the Northeast of Turbe Tepe (Figure 2b). Moreover, many networks of fractures overlain by Neojen deposits resembling these faults have been found in the investigated area and have also been noticed in the radargrams.

The locations of massive blocks of marble and the distribution of structural discontinuities are indicated by continuous lines and boxes (Figure 8). With such useful information, the quarry operators will know whether this area is exploitable or not and the quarrying will be more cost-effective. Given that quarries in neighboring areas had to be closed down because of the presence of a dense network of discontinuities in the marble, and considering the results of our study, the proprietors of this quarry decided that no quarrying activity could be started in the study area.

ACKNOWLEDGEMENTS

Many thanks to Ankara Makro Mermer for the continued help during field work and Burak Yıldırım, a student at Geophysics Department, Karadeniz Technical University. We are also grateful to Dr. Bulent Yalcinalp, Dr. Raif Kandemir and Dr. Hakan Ersoy for compiling the geological information, Dr. Hakan Karsli for his contribution in the advancement of data processing stages and Melek Demir for the translation part.

REFERENCES

Acikgoz AD (2008). Investigation of cracked-fractured systems in marble site (Haymana-Ankara) using by ground penetrating radar (Bir mermer sahasında (Haymana/Ankara) yer radarı yöntemi ile kırık-çatlak sistemlerinin araştırılması). MSc thesis, Karadeniz Technical University, Trabzon, Turkey.

Annan AP (2003). Ground-penetrating radar principles, procedures and applications. Sensors & Software Inc., Canada.

Arcone SA, Lawson DE, Delaney AJ, Strasser JC Strasser JD (1998). Ground-penetrating radar reflection profiling of groundwater and bedrock in an area of discontinuous permafrost. Geophysics, 63: 1573–1584.

Daniels DJ (2004). Ground penetrating radar. 2nd edition. The Institution of Electrical Engineers.

Daniels JJ (1996). Surface Penetrating Radar. The Institution of Electrical Engineers, London, United Kingdom.

Davis JL, Annan AP (1989). Ground penetrating radar for high resolution mapping of soil and rock stratigraphy. Geophys. Prospect. 37: 531–551.

Deparis J, Fricout B, Jongmans D, Villemin T, Effendiantz L, Mathy A (2008). Combined use of geophysical methods and remote techniques for characterizing the fracture network of a potentially unstable cliff site (the 'Roche du Midi', Vercors massif, France). J. Geophys. Eng. 5: 47-157.

Gelchinsky BY, Landa E, Shtivelman V (1985). Algorithms of phase and group correlation. Geophysics 50: 596–608.

Grandjean G, Gourry JC (1996). GPR data processing for 3D fracture mapping in a marble quarry (Thassos, Greece). J. Appl. Geophys. 36: 19-30.

Grasmueck M (1996). 3D ground penetrating radar applied to fracture imaging in gneiss. Geophysics, 61(4): 1050–1064.
Grasmueck M, Weger R, Hortsmeyer H (2005). Full-resolution 3D GPR imaging. Geophysics, 70: K12-K19.
Jeannin M, Garambois S, Jongmans D, Gr´egoire C (2006). Multiconfiguration GPR measurements for geometric fracture characterization in limestone cliffs (Alps). Geophysics, 71: B85–92.
Jol MH (2009). Ground penetrating radar theory and applications, Elsevier Science, The Netherlands.
Kadioglu S (2008). Photographing layer thicknesses and discontinuities in a marble quarry with 3D GPR visualization. J. Appl. Geophys. 64: 109-114.
Karsli H (2002). Evaluation of stacked seismic traces with complex trace analysis in terms of resolution. Earth Sci. 26: 15-26.
Karsli H, Dondurur D, Çifçi G (2006). Application of complex-trace analysis to seismic data for random-noise suppression and temporal resolution improvement. Geophysics, 71: V79-V86.
Kim JH, Cho SJ, Yi MJ (2007). Removal of ringing noise in GPR data by signal processing. Geosci. J. 11: 75−81.
Olhoeft GR (1981). Electrical properties of rocks, in physical properties of rocks and minerals, edited by Y.S. Touloukian, C.Y. Ho and R.F. Roy, McGraw-Hill, New York, pp. 257-329.
Orlando L (2003). Semiquantitative evaluation of massive rock quality using ground penetrating radar. J. Appl. Geophys. 52: 1–9.
Patterson JE, Cook AF (2000). The application of complex trace analysis for improved target identification in GEM tourmaline bearing pegmatites Himalaya Mine, San Diego County, California. GPR 2000: Proceedings of the Eighth İnternational Conference on Ground Penetrating Radar: Gold Coast, 23-26 May.
Porsani JL, William AS, Abad OSJ (2006). GPR for mapping fractures and as a guide for the extraction of ornamental granite from a quarry: A case study from southern Brazil. J. Appl Geophys. 58: 177-187.
Sandmeier KJ (2009). Reflexw 5.0.5 manual. Sandmeier Software, Zipser Strabe 1, D-76227 Karlsruhe, Germany.
Seol SJ, Kim JH, Song Y, Chung SH (2001). Finding the strike direction of fractures using GPR. Geophys. Prospect. 49: 300–308.
Shaffer NR, Wenning AL (2002). Ground Penetrating Radar (GPR) in Industrial Mineral Mining, North-Central Section (36th) and Southeastern Section (51st). GSA Joint Annual Meeting, Economic Geology.
Shtivelman V, Landa E, Gelchinsky BY (1986). Phase and group time sections and possibilities for their use in seismic interpretation of complex media. Geophys. Prospect. 34: 508–536.
Tillard S (1994). Radar experiments in isotropic and anisotropic geological formations granite and schists. Geophys. Prospect. 42: 615–636.
Tsoflias GP, Gestel JPV, Stoffa PL, Blankenship DD Sen M (2004). Vertical fracture detection by exploiting the polarization properties of ground-penetrating radar signals. Geophysics, 69: 803-810.
Ünalan G, Yüksel V, Tekeli T, Gönenç O, Seyirt Z, Hüseyin S (1976). Paleogeographical evolution and Upper Cretaceous-Lower Tertiary stratigraphy of Haymana-Polatlı region (southwest of Ankara) (Haymana-Polatlı yöresinin (güneybatı Ankara) Üst Kretase-Alt Tersiyer stratigrafisi ve paleocoğrafik evrimi), Türkiye Jeoloji Kurumu Bülteni, 19: 159-176.